CRYSTAL GROWTH & DESIGN
XXXX
VOL. 0, NO. 0
1−6

Identification of Mineral Modulation Sequences within the Nacre-Associated Oyster Shell Protein, n16

Il Won Kim,[†] Elaine DiMasi,[‡] and John Spencer Evans*,[†]

Laboratory for Chemical Physics, New York University, 345 East 24th Street, New York, New York, 10010, and Department of Physics, Brookhaven National Laboratory, Upton, New York, 11973-5000

Received February 27, 2004

ABSTRACT: Nature's use of proteins to direct and control the synthesis of inorganic solids represents an important paradigm for bioinspired materials synthesis. However, the mechanism by which polypeptides direct inorganic synthesis, particularly with regard to selective formation of crystals polymorphs, remains unknown. An important step in understanding polypeptide-directed inorganic synthesis is the identification of sequence regions in biomineralization proteins that can affect crystal growth. In this report, we identify that the 30 AA N- and C-terminal sequence regions (n16-N and n16-C, respectively) of the oyster shell aragonite-associated protein, n16, exhibit control over the morphology of calcium carbonate crystals grown in geologic calcite overgrowth assays and polyimide (Kevlar)-based assays. Here, we find that calcium carbonate crystals, which grow in the presence of model peptides representing the n16-N and n16-C sequences, adopt dendritic or circular overgrowth in geological calcite overgrowth assays and "staircase" structures in Kevlar-based assays, as compared to negative controls and to parallel assays conducted in the presence of AP24-1, the 30 AA N-terminal sequence region of the nacre-associated protein, AP24, which interrupts step edge growth. Synchrotron X-ray diffraction studies reveal that the crystals grown in the presence of n16-N are calcite. Circular dichroism spectrometry studies of n16-N and n16-C model peptides reveal qualitatively similar solution state conformations that consist of either random coil in equilibrium with other secondary structures (e.g., β-strand, turn, loop, polyproline type II) or, at higher concentrations, a β-strand secondary structure in equilibrium with random coil. We conclude that the N- and C-terminal sequence regions of the nacre-associated n16 protein most likely play a role in n16-mediated effects on calcium carbonate crystal growth in the nacre layer.

Nature's use of proteins to regulate the growth of inorganic solids is one of the major hallmarks of the biomineralization process and represents one possible pathway for the construction of unique and useful inorganic materials. A great deal of interest has centered on calcium carbonate-based mineralization processes, where several crystalline polymorphs (calcite, aragonite, and vaterite) and amorphous calcium carbonates are preferentially created within certain organisms.[1] An interesting model system of polymorph selection exists in the mollusk shell, where two polymorphs, calcite (prismatic layer) and aragonite (nacre layer), coexist side by side.[2−7] Recent protein studies have identified a number of unique polypeptides associated with the nacre layer,[5,6,9] and it is believed that these proteins participate in the stabilization of the aragonite polymorph during shell synthesis.[3−8] Thus, if one is interested in exploiting the principles of bioinspired inorganic synthesis and protein-mediated phase stabilization for material science,[10] we need to obtain a better understanding of how these proteins affect mineral formation at the molecular level.

One piece of the puzzle may reside within the primary sequence and conformation of protein domains which affect calcium carbonate polymorphisms. Recent multidisciplinary studies of a series of nacre-associated proteins (e.g., AP7,[5] AP24,[5] and Lustrin A[11]) reveal a trend with regard to the types of sequence motifs that affect calcium carbonate mineralization. In particular, these three proteins contain at least one mineral interaction or modifying domain that possess the following attributes:[5,11−13] (i) a limited occurrence (10−25% of the domain sequence) of anionic amino acids (Asp and Glu); (ii) a copolymer block-like arrangement of hydrogen-bonding or proton donor/acceptor amino acids (e.g., His, Gln, Asn, Tyr, Ser, His, Arg, and Lys); and (iii) the presence of unfolded or labile/unstable conformation within the mineral-associated sequence domain, as determined by NMR and/or circular dichroism (CD) spectroscopy. These molecular traits are also shared by the C-terminal domain of the calcium carbonate-associated protein, lithostathine,[14] and may represent key requirements for a polypeptide domain that controls calcium carbonate mineralization.[12]

To determine whether these molecular attributes extend to sequence domains within other nacre-associated proteins, we have explored a series of nacre proteins which have been implicated in the formation of aragonite. In particular, one protein, n16 (108 AA, nonglycosylated), has been isolated from the nacre layer of the Japanese pearl oyster, *Picntada fucata*, and sequenced.[9] Preliminary in vitro assay studies indicated that the n16 protein can induce the formation of either spherical or platelike crystals, and under certain conditions, aragonite mineral deposits have been observed.[9] Intriguingly, an examination of the n16 primary sequence[9] reveals that the 30 AA N- and C-terminal sequence regions of the mature, posttranslationally cleaved protein possess the requisite amino acids associated with a calcium carbonate mineral modification domain:

N-terminal (n16-N, sequence 1−30)
AYHKKCGRYSYCWIPYDIERDRYDNGDKKC...

C-terminal (n16-C, sequence 79−108) ...
GLNYLKSLYGGYGNGNGEFWEEYIDERYDN

To ascertain if these two terminal sequence regions affect calcium carbonate crystal growth, we constructed synthetic peptides representing n16-N and n16-C and tested these two sequences alongside the 30 AA calcite growth step inhibitor polypeptide, AP24-1.[5] These peptide sequences were tested in calcium carbonate crystal growth assays

* To whom correspondence should be addressed. E-mail: jse1@nyu.edu.
[†] New York University.
[‡] Brookhaven National Laboratory.

10.1021/cg049919a CCC: $27.50
Published on Web 00/00/0000

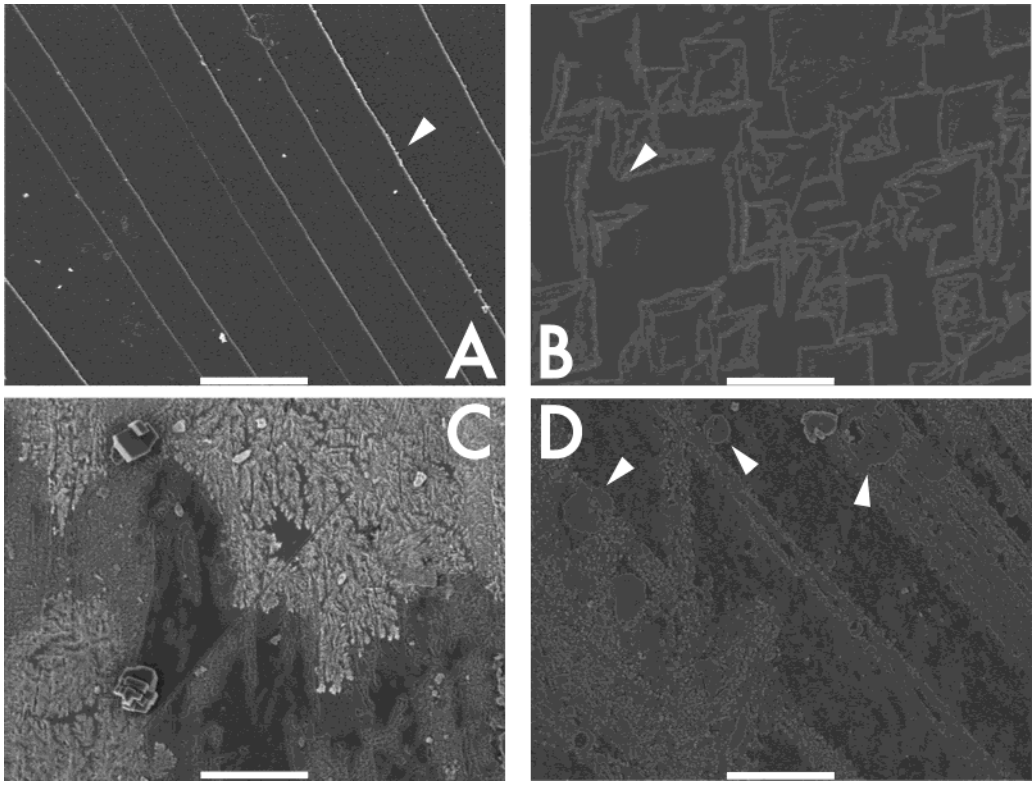

Figure 1. Scanning electron microscopy images of in vitro geologic overgrowth calcium carbonate assay systems. (A) Negative control assay. Dark regions represent normal crystal overgrowth regions that are delineated by step edge boundaries (denoted by white arrow). (B) AP24-1, 3.3×10^{-5} M peptide. Here, normal overgrowth regions appear dark, and areas where overgrowth is inhibited appear light and feature irregular boundaries (white arrow). (C) n16-N, 3.3×10^{-5} M peptide. Dendritic crystal formation (light) is observed to occur on the surface of normal overgrowth regions (in dark). (D) n16-C, 3.3×10^{-5} M peptide. Multiple, rounded, rhombohedral crystal overgrowth is observed on the surface of normal overgrowth regions, and in addition, pseudo-circular crystal overgrowth is also observed (denoted by white arrows). Scale bar = 10 μm.

employing either Iceland spar geological calcite fragments[5,7] (overgrowth assay) or synthetic polyimide fibers[15,16] (Kevlar-based assay, $(NH_4)_2CO_3$ decomposition[17]) to induce crystal formation in the presence of each peptide (tested concentration range = 3.3×10^{-6} to 1.7×10^{-4} M in each assay). We find that as compared to control conditions, n16-N and n16-C exert a similar effect on the formation of calcium carbonate crystals in both in vitro assays systems. Moreover, using CD spectrometry, we observe that both polypeptides, although different in their primary sequence, feature similar concentration-dependent conformations in solution (a β-strand in equilibrium with a random coil).

Peptide Synthesis and Purification. The 30-mer polypeptide, n16-N, representing the 1−30 AA domain of native n16, was synthesized using the protocol described in our earlier work (100 μmol synthesis level).[5] This peptide featured free amino termini and C^{α} amide "capping" to mimic its attachment to the protein and negate the charge contribution from the α-carboxylate C terminus. Similarly, N-acetyl-capped, free carboxylate 30 AA terminus n16-C was also synthesized and purified in a similar fashion.[5] After resin cleavage and reverse phase high-performance liquid chromatography purification (C-18 column, >94% pure for all peptides),[5] the experimental molecular masses for n16-N and n16-C were determined by matrix-assisted laser desorption/ionization time-of-flight mass spectrometry to be 3748.5 and 3579.2 Da, respectively, in agreement with the theoretical molecular masses of 3747.2 and 3579.8 Da. The 30 AA AP24-1 C^{α} amide-capped, free N terminus polypeptide representing the N-terminal sequence of the calcite growth step inhibitor protein, AP24-1,[5] was synthesized and purified as described.[5]

In Vitro Calcium Carbonate Mineralization Assays and SEM Analyses. To investigate the effects of n16-C and n16-N polypeptide sequences on the growth of $CaCO_3$, two different crystal growth assays systems were employed. The first, the calcite overgrowth assay,[5,7] involved the use of freshly cleaved crystals of geological calcite (Iceland spar) measuring approximately 5−8 mm on edge and 1−2 mm in thickness. These fragments were placed in 3 mL of growth solution (12.5 mM $CaCl_2 \cdot 2H_2O$, 12.5 mM NH_4HCO_3, Aldrich-Sigma) in borosilicate glass screw cap vials.[5] The purified polypeptides were dissolved in deionized distilled water to a final concentration of 1 mM, and the pH of these peptide stock solutions was adjusted to 7.5 using NaOH. A concentration series (final concentrations of 3.3×10^{-6}, 1.7×10^{-5}, 3.3×10^{-5}, and 1.7×10^{-4} M peptide/vial) of n16-C, n16-N, and AP24-1 were incubated in each sealed vial for 90 min at 15 °C. The negative control conditions consisted of no added peptide. At the conclusion of the incubation period, the supernatant was removed via suction and the calcite crystals were washed three times with 3 mL volumes of calcium carbonate-saturated methanol and then dried at 37 °C.

To complement the geological calcite overgrowth assays, we also employed the polyimide (Kevlar) fiber assay for template growth of calcium carbonate crystals[15,16] in the presence of model peptides. The published Kevlar technique[15] was modified and optimized for use with polypeptides in the following manner. First, Kevlar-29 fiber mats (DuPont, United States, 0.5 mm individual fiber diameter) were teased into individual fibers and these individual fibers were then cut into approximately 1 cm lengths. All manipulations of fibers from this point on were done using nylon-tipped tweezers. These fibers were washed five times

with 50%/50% v/v acetone/methanol to clean off any residual organic material, finger oils, etc. and then air-dried at 37 °C. The fibers were then treated with 3 N HCl in deionized distilled water for 6 h at room temperature to enhance the charge and polarity at exposed Kevlar surfaces (i.e., promote amide bond cleavage and exposure of carboxylate and amine groups).[15,16] These treated fibers were then rinsed extensively with deionized distilled water and dried at 37 °C and stored in a sealed desiccator (Drierite) until needed. For the assay, clean, HCl-treated fibers were submerged in polystyrene Petri dishes containing 3 mL of 10 mM $CaCl_2 \cdot 2H_2O$ in deionized distilled water plus the appropriate volume of peptide stock solutions to create the final peptide assay concentrations of 1.7×10^{-5}, 3.3×10^{-5}, and 1.7×10^{-4} M peptide/dish. The negative control conditions consisted of no added peptide. A pinhole opening (1−2 mm) was introduced in the top of each Petri dish cover. The Petri dishes were then incubated at 15 °C for 16 h in a sealed chamber (1 L volume) containing 2 g of solid $(NH_4)_2CO_3$ (Sigma-Aldrich, decomposition vapor method).[17] At the conclusion of the assay periods, the assay supernatants were removed via aspiration and the Kevlar fibers were gently washed three times with 3 mL volume each of calcium carbonate-saturated methanol and then dried at 37 °C.

Both geologic and Kevlar samples were mounted on carbon conductive scanning electron microscopy (SEM) tabs placed on aluminum SEM holders and sputter coated with Pt/Pd (argon-flushed vacuum chamber) for 4 min. SEM imaging was conducted using an AMRAY FE-1850 cathode field emission microscope operating at 5 kV and equipped with a charge-coupled device (CCD) detector for image capture. Cropping of the SEM images and adjustment of brightness/darkness and contrast levels were performed using Adobe Photoshop.

X-ray Diffraction. Crystals formed by Kevlar-based assays treated with n16-N were studied at the National Synchrotron Light Source Beamline ×6B using an X-ray wavelength of 0.689 Å and a MARCCD detector. The Kevlar fibers with adhering $CaCO_3$ crystals were inserted into thin-walled glass capillaries and rotated about the capillary axis during data acquisition. Geological calcite overgrowth assays containing n16-N (data not shown) were studied at NSLS Beamline ×22A and were mounted with the beam incident below the critical angle for total external reflection to enhance the signal from the surface region.

CD Spectrometry. For CD studies, lyophilized n16-N and n16-C were dissolved in either 100 μM NaH_2PO_4, pH 2.5, or 100 μM Tris-HCl, pH 7.5, buffers to create final polypeptide concentrations of 500 μM. These polypeptide stock solution were then diluted to 25, 15, 10, 8, 4, and 2 μM in the appropriate buffer for CD spectrometry measurements at pH 2.5 and 7.5. The CD spectra were obtained using an AVIV 60 CD Spectrometer, running 60DS software version 4.1t. The peptide samples were scanned from 185 to 260 nm at 25 °C, using 1 nm bandwidth and a scan rate of 1 nm/s, with appropriate background buffer subtraction performed. The spectrometer was previously calibrated with d-10-camphorsulfphonic acid. A total of three scans were acquired for each aqueous peptide sample. The mean residue ellipticity $[\theta_M]$ is expressed in deg cm^2 dmol^{-1} per mole peptide.

Crystal Growth Assays. As compared to negative control conditions (i.e., no peptide present; Figure 1A), geologic calcite overgrowth assays containing the growth step inhibitor polypeptide, AP24-1 (Figure 1B), reveal the typical step edge interruption or frustration of crystal growth associated with this polypeptide. Although clear rhombohedral terraces are retained in the overgrowth regions (dark contrast), they are reduced to <10 μm extent. Step edges appear rounded or irregular, indicating the partial adsorption of this polypeptide to step edges.[5] In the presence of n16-N, any rhombohedral step morphology, if present, is reduced below the 100 nm length scale. Instead, we observe calcium carbonate overgrowth that features dendrite crystallization superimposed upon the overgrowth surface (Figures 1C and 2A). Similar crystallization patterns have been noted for block copolymer protein-mediated inorganic and organic crystal formation in vitro[18] and have long been attributed to the adsorption of additives at exposed crystal surfaces and/or step edges,[19,20] apparently occurring at a significant coverage as compared to AP24-1. Similarly, the presence of n16-C also restricts the rhombohedral morphology to small length scales (Figure 1D). With this sequence, some overgrowth step edges are visible, which reproduce the alignment of the single-crystal calcite substrate, but we also observe regions that are rounded on micrometer and submicrometer scales (Figure 2B; note arrows). The presence of step edges is typical of calcium carbonates;[20] however, it should be noted that at this time we cannot verify that the circular and dendrite crystal growth regions produced by n16-N and n16-C are comprised solely of calcium carbonate. It is possible that these growth regions contain some content of adsorbed polypeptide as well.

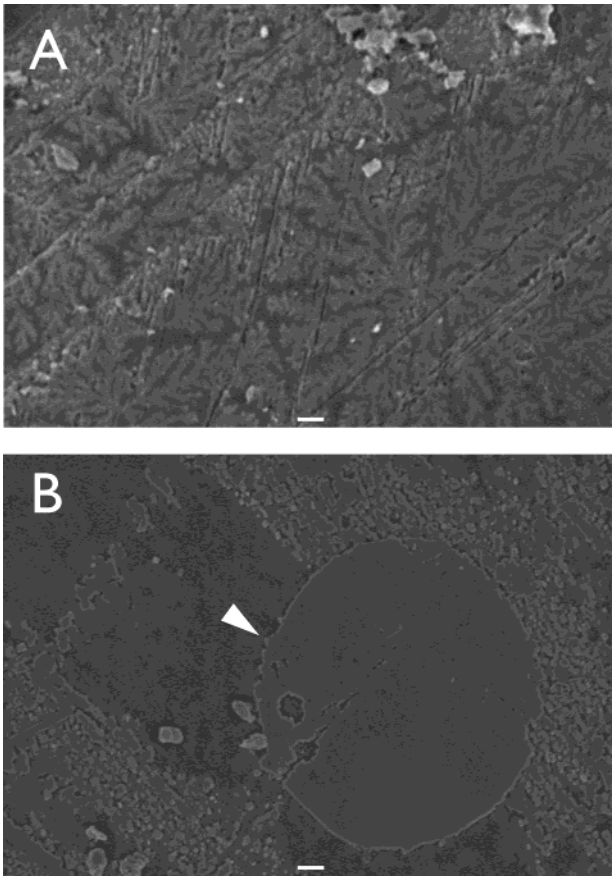

Figure 2. Higher magnification scanning electron microscopy images of in vitro geologic overgrowth calcium carbonate assay systems. (A) n16-N, 3.3×10^{-5} M peptide. Here, the dendritic crystal growth is clearly seen on the overgrowth surfaces. (B) n16-C, 3.3×10^{-5} M peptide. Arrows denote the presence of step edge regions. Scale bar = 1 μm.

These polypeptide specific crystal growth effects are also mirrored in Kevlar-based calcium carbonate crystal growth assays (Figure 3). Calcite has four step directions on the low-energy {104} face,[20] which is what we primarily

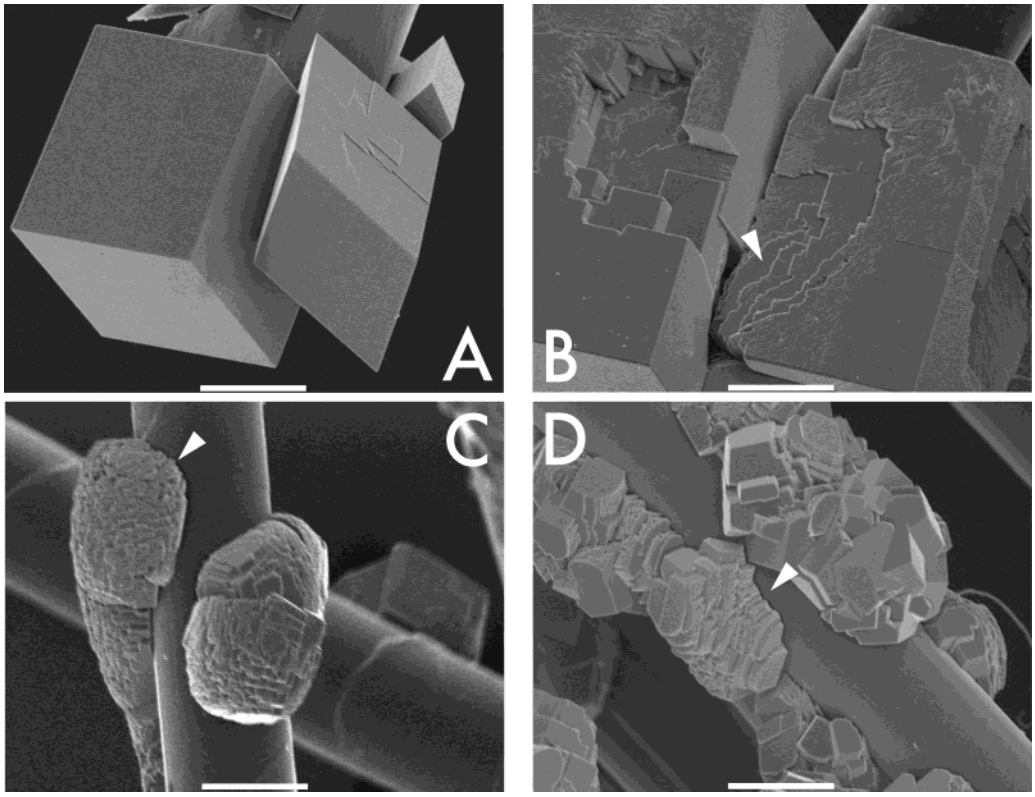

Figure 3. Scanning electron microscopy images of in vitro Kevlar calcium carbonate assay systems. (A) Negative control assay, which features typical rhombohedral calcite crystals. (B) AP24-1, 1.7×10^{-4} M peptide, where rhombohedral calcite crystals featuring interruptions in crystal growth and irregular step edges (white arrow) are seen. (C) n16-N, 1.7×10^{-4} M peptide, where the appearance of stairlike structures on exposed surfaces is evident (white arrow). (D) n16-C, 1.7×10^{-4} M peptide, where crystals exhibit an overall, rounded, rhombohedral shape and feature stairlike crystal structures (white arrow). Scale bar = 10 μm.

observe in our SEM images of negative control crystals (Figure 3A). Two of the steps form an acute angle with respect to the surface plane, and the other two form an obtuse angle with respect to the surface plane.[20] Assays conducted in the presence of AP24-1 feature comparably sized rhombohedral calcite crystals that possess interruptions in crystal growth as well as rounded step edge regions (Figure 3B), in accord with the expected function of the parent protein, AP24, which interacts at growth step edges.[5] In the case of n16-N (Figure 3C), we observe that the forming calcite crystals do not retain any of their sharp corner features in the presence of this polypeptide. Instead, these calcium carbonate crystals feature multiple step edges where both the acute and the obtuse surface steps appear to be affected, leading to the formation of "staircase structures" that have small terrace sizes. n16-C by contrast appears to preferentially interact with the two acute surface steps and less so with the obtuse surface steps (Figure 3D), since the resulting crystals retain their sharp corner features where the three faces intersect and the obtuse surface steps appear smooth. Nevertheless, calcium carbonate crystals that grow in the presence of n16-C also adopt staircase structures, with closely spaced step edges similar to those observed for n16-N. From these results, we conclude that n16-N and n16-C affect calcium carbonate crystal growth in a different manner from the growth step inhibitor polypeptide sequence, AP24-1. Obviously, more precise imaging techniques, such as atomic force microscopy, will be required to more fully determine with which surfaces these polypeptide sequences interact.

As shown in Figure 3D, the morphology of the calcium carbonate crystals that grow in the presence of n16-C appear to be that of calcite, based upon the rhombohedral-like morphology presented. However, because of the presence of staircase structures (Figure 3C) and loss of typical calcite features, it is not clear what the corresponding crystal polymorph may be in the presence of n16-N. To determine the lattice structure of the more unusual calcium carbonate crystals grown on Kevlar surfaces in the presence of n16-N, we examined these small Kevlar assay crystals using synchrotron X-ray diffraction (Figure 4). Diffraction patterns obtained matched those of calcite, with no evidence of peaks specific for either vaterite or aragonite.[15−17] Geological calcite overgrowth fragments from n16-N-treated assays were also sampled using synchrotron surface X-ray scattering techniques, but again, only peaks belonging to the calcite spectrum were observed (data not shown). Thus, using two different in vitro crystal growth assays, we find that both the n16-N and the n16-C sequence regions possess the capability of modifying the morphology of calcium carbonate crystals. However, at this time, the only detectable polymorph observed to form under the conditions utilized in both assay systems is calcite.

CD Spectrometry. In previous studies of mineral modification domains in the nacre specific proteins, AP7 and AP24, it was noted that there were certain preferences for unfolded, conformationally labile conformations in solution.[5,13] To ascertain what conformational preferences the terminal sequences of n16 may possess, we qualitatively investigated the secondary structure preferences for both n16 terminal sequences via CD spectrometry (Figure 5). At neutral pH, both polypeptides exhibit interesting concentration-dependent conformations. At 4 μM peptide concentration, we observe broad (−) CD absorption bands centered at 199−200 nm ($\pi-\pi^*$ transition). These bands are consistent with the presence of a random coil conformation that exists in equilibrium with other secondary structures such as turn, loop, polyproline type II, and

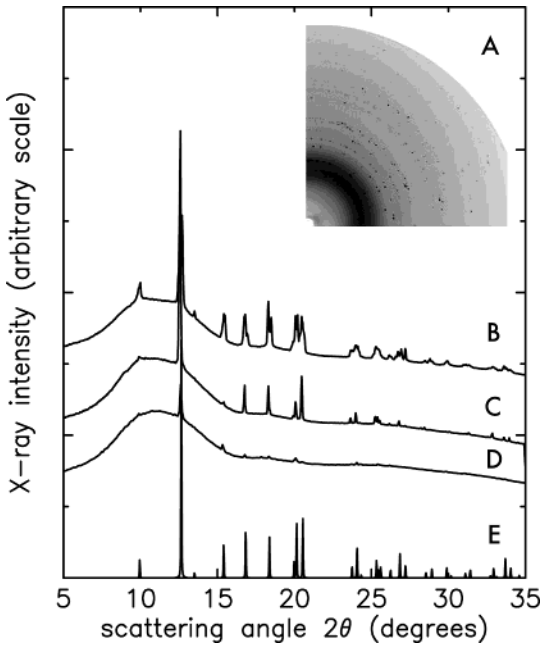

Figure 4. Synchrotron X-ray scattering from Kevlar-templated negative control and n16-N-treated calcium carbonate crystals. (A) Representative raw 2D detector data showing the coarse powder of crystals associated with the Kevlar fibers. The diffuse band near the center is scattering from the glass capillary sample holder. Scattering from the Kevlar (studied separately with a clean Kevlar sample, not shown) lies along the horizontal and vertical axes, and these regions were avoided in the azimuthal averages shown in B−D. (B, C) Calcium carbonate crystals obtained from n16-N Kevlar assay (1.7×10^{-4} M peptide). (D) Negative control. (E) Computed calcite diffraction pattern.

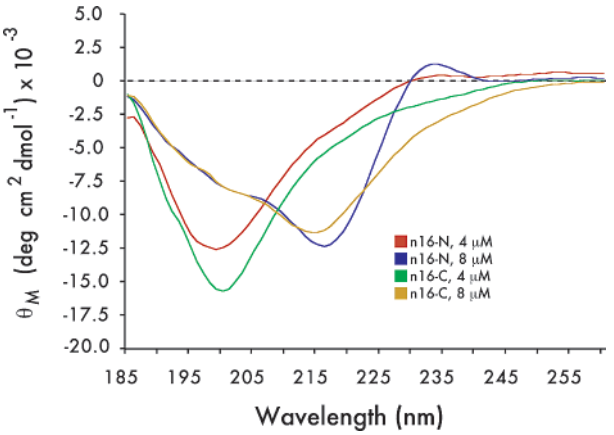

Figure 5. CD spectra of n16-N and n16-C polypeptides at 4 and 8 μM concentrations in 100 μM Tris-HCl, pH 7.5, in deionized distilled water at 25 °C.

β-strand.[5,21−23] However, when the peptide concentrations are raised to 8 μM (Figure 5), we obtain CD spectra that feature two bands: one, a weak (−) CD absorption band centered at 201 nm ($\pi-\pi^*$ transition) corresponding to the presence of random coil,[5,24−26] and a strong (−) CD absorption band centered at 215 nm ($n-\pi^*$ transition) that is consistent with the presence of a β-strand conformation.[26] Note also that the n16-N polypeptide exhibits a third (+) CD adsorption band centered at 233 nm. The presence of $\pi-\pi^*$ (201 nm) and $n-\pi^*$ (215 nm) transition bands was also noted for both polypeptides at concentrations >8 μM (data not shown). Similarly, the presence of a conformational shift was also replicated at pH 2.5 for both polypeptides (data not shown).

We attribute the observed n16-N and n16-C concentration-dependent conformational shift to some degree of interchain peptide self-association or stabilization in solution at 8 μM or higher concentrations that does not occur at more dilute concentrations. Similar concentration-dependent results were recently obtained for synthetic peptides derived from the β-sheet domain of platelet factor 4 and were attributed to gelation effects.[27] Note that the concentration-dependent conformational switching was not observed for the calcium carbonate step edge inhibitory sequences, AP24-1 and AP7-1. Both of these step edge inhibitor sequences possess a random coil-like conformation (i.e., single broad absorption band representing the $\pi-\pi^*$ transition, centered at 199−200 nm) at 8 πM[5] and feature open, unfolded structures at neutral pH as demonstrated by solution state NMR at 850 μM.[13] Thus, depending upon the concentration, n16-N and n16-C polypeptide sequences can exist either as unfolded, random coil-like molecules or in a conformational equilibria consisting of some mixture of random coil-like and β-strand conformers. At this time, we do not know what the impact of the concentration-dependent structure has on our assay system data (where n16-N and n16-C concentrations = 33 and 170 μM) nor on the actual events that take place with the n16 protein during nacre mineralization.

Our findings indicate that the n16 protein possesses N- and C-terminal domains that can affect the morphology of calcium carbonate crystals in vitro. We also note that both terminal sequences are qualitatively similar in structure and exhibit an interesting and previously unpublished concentration-dependent conformational switching effect. From our SEM data, we conclude that the N- and C-terminal sequence regions probably play some role in the ability of n16 to control calcium carbonate crystal formation within the nacre layer of the oyster shell,[9] although it is not known which calcium carbonate polymorph (ACC, vaterite, calcite, or aragonite) n16 interacts with in vivo. Obviously, other sequence regions within n16 may also contribute to the overall protein-mediated calcium carbonate modulation and these will be explored in time.

We should note that our study has raised some interesting issues regarding the mechanism of n16-N and n16-C modulation of calcium carbonate crystal growth. From the Kevlar data (Figure 3), it appears that the observed effects may arise from direct peptide interactions with exposed acute and/or obtuse surface steps.[11,20] However, our study cannot rule out the possibility that the observed morphology changes arise from peptide-catalyzed solution-mediated effects, e.g., proton transfer, ion cluster formation, or water binding that occurs on the exposed surfaces of the polypeptides in the vicinity of the growing crystal interfaces. Second, although concentration-dependent conformational switching is observed for n16-N and n16-C, it is not clear if this switching arises from intermolecular self-association processes in each polypeptide or intramolecular folding that is mediated by polypeptide concentration. Moreover, the impact of this conformational switching on in vitro crystal growth or on events related to n16 protein participation in nacre mineralization is not clearly understood at this time and must await additional experimentation for clarification.

In this study, we observe that two terminal mineral modification sequences derived from a single parent protein can generate effects on calcium carbonate crystal formation in vitro. Depending upon the assay system, these effects appear to be either quite different (Figures 1 and 2) or very similar (Figure 3), but they do not appear to be identical. This result can be interpreted in at least two ways. First, it may indicate that like other reported biomineralization

proteins, the n16 protein may have evolved distinct sequence domains with different functionalities,[28] as witnessed by the fact that n16-N and n16-C possess different primary sequences.[9] Hypothetically, it is possible that each sequence domain evolved a slightly different functionality when it comes to mediating calcium carbonate crystal growth, e.g., different preferences for calcium carbonate surfaces (Figure 3). Alternatively, the differences in observed function may be artifactual and related to our arbitrary criteria of 30 AA sequence length for each polypeptide in this study. It may be that the true sequence lengths of each mineral modification domain are different from those selected in this study and that the proper sequence lengths may lead to identical assay results in vitro. To ascertain if the latter is a possibility, we are currently exploring the effect of sequence extension/truncation on n16-N and n16-C function in vitro. These results will be reported elsewhere.

Finally, a comparison of the n16-N and n16-C sequences with the calcium carbonate growth step inhibitor sequences, AP7-1 and AP24-1, reveals some interesting similarities and contrasts. First, the AP7-1 and AP24-1 polypeptides adopt unfolded, labile conformations that consist of random coil, extended structure, and loop regions,[13] and these sequences interrupt crystal growth at step edge regions[5] but have not been observed to produce dendrite or circular calcium carbonate crystals (Figures 2 and 3).[5] As demonstrated in this article, the n16-N and n16-C polypeptides, although possessing nonidentical primary sequences, also possess labile, unfolded conformations as well. However, unlike AP7-1 and AP24-1, the conformational equilibria for both terminal sequences of n16 appear to be concentration-dependent and are observed to vary from predominantly random coil-like (i.e., unfolded and conformationally labile) to some equilibrium mixture of random coil state and β-strand secondary structure (Figure 5). Likewise, n16-N and n16-C sequences do not generate step edge interruption effects such as those observed for AP7-1 and AP24-1. Rather, it appears that n16-N and n16-C inhibit calcium carbonate growth in a different fashion from the N-terminal sequences of AP7 and AP24. Finally, there are interesting compositional differences: both n16-N and n16-C sequences possess a single Trp residue, whereas Trp does not appear in either the AP7-1 or the AP24-1 sequences.[5] Conversely, Thr and Gln appear in both the AP7-1 and the AP24-1 sequences but are not present in either n16-N or n16-C. At this time, it is not entirely clear what amino acid compositional or primary sequence factors are essential for interaction or mediation of calcium carbonates, nor how secondary structure or conformational lability/equilibria play a role in polypeptide−inorganic interactions. Experiments are currently in progress to determine the participation of specific amino acids and the effect of polypeptide structure on crystal growth.

Acknowledgment. This work was supported by funding from the Department of Energy (DE-FG02-03ER46099, to J.S.E.) and represents contribution number 25 from the Laboratory for Chemical Physics, New York University. The National Synchrotron Light Source is supported under U.S. DOE Contract DE-AC02-98CH10886. We thank Dr. Paul Heiney of Datasqueeze Software, Inc., for making Datasqueeze available for analysis of the diffraction patterns.

References

(1) Lowenstam, H. A.; Weiner, S. *On Biomineralization*; Oxford Press: New York, 1989.
(2) Cariolou, M. A.; Morse, D. *J. Comp. Physiol. B* **1988**, *157*, 717−729.
(3) Fritz, M.; Belcher, A. M.; Radmacher, M.; Walters, D. A.; Hansma, P. K.; Stucky, G. D.; Morse, D. E.; Mann, S. *Nature* **1994**, *371*, 49−51.
(4) Belcher, A. M.; Wu, X. H.; Christensen, R. J.; Hansma, P. K.; Stucky, G. D.; Morse, D. E. *Nature* **1996**, *381*, 56−58.
(5) (a) Michenfelder, M.; Fu, G.; Weaver, J. C.; Wustman, B. A.; Taranto, L.; Evans, J. S.; Morse, D. E. *Biopolymers* **2003**, *70*, 522−533. (b) Michenfelder, M.; Fu, G.; Weaver, J. C.; Wustman, B. A.; Taranto, L.; Evans, J. S.; Morse, D. E. *Biopolymers* **2004**, *73*, 299.
(6) Falini, G.; Albeck, S.; Weiner, S.; Addadi, L. *Science* **1996**, *271*, 67−69.
(7) Thompson, J. B.; Paloczi, G. T.; Kindt, J. H.; Michenfelder, M.; Smith, B. L.; Stucky, G.; Morse, D. E.; Hansma, P. K. *Biophys. J.* **2000**, *79*, 3307−3312.
(8) Walters, D. A.; Smith, B. L.; Belcher, A. M.; Paloczi, G. T.; Stucky, G. D.; Morse, D. E.; Hansma, P. K. *Biophys. J.* **1997**, *72*, 1425−1433.
(9) Samata, T.; Hayashi, N.; Kono, M.; Hasegawa, K.; Horita, C.; Akera, S. *FEBS Lett.* **1999**, *462*, 225−229.
(10) Sarikaya, M.; Tamerler, C.; Jen, A. K.-Y.; Schulten, K.; Baneyx, F. *Nat. Mater.* **2003**, *2*, 577−585.
(11) (a) Wustman, B. A.; Weaver, J. C.; Morse, D. E.; Evans, J. S. *Langmuir* **2003**, *19*, 9373−9381. (b) Wustman, B. A.; Weaver, J. C.; Morse, D. E.; Evans, J. S. *Langmuir* **2004**, *20*, 277.
(12) Evans, J. S. *Curr. Opin. Colloid Interface Sci.* **2003**, *8*, 48−54.
(13) Wustman, B. A.; Morse, D. E.; Evans, J. S. *Biopolymers* **2004**, *74*, 363−376.
(14) Gerbaud, V.; Pignol, D.; Loret, E.; Bertrand, J. A.; Berland, Y.; Fontecilla-Camps, J.-C.; Canselier, J.-P.; Gabas, N.; Verdier, J.-M. *J. Biol. Chem.* **2000**, *275*, 1057−1064.
(15) Lakshminarayanan, R.; Valiyaveettil, S.; Loy, G. L. *Cryst. Growth Des.* **2003**, *3*, 953−958.
(16) Kato, T.; Amamiya, T. *Chem. Lett.* **1999**, *3*, 199−200.
(17) Kim, I. W.; Robertson, R. E.; Zand, R. *Adv. Mater.* **2003**, *15*, 709−713.
(18) Shiba, K.; Honma, T.; Minamisawa, T.; Nishiguchi, K.; Noda, T. *EMBO Rep.* **2003**, *4*, 148−153.
(19) Walton, A. G. *The Formation and Properties of Precipitates*; Interscience Publishers: New York, 1967; Chapter 5.
(20) DeYoreo, J. J.; Vekilov, P. G. Principles of crystal nucleation and growth. *Reviews in Mineralogy and Geochemistry: Biomineralization*; The Mineralogical Society of America, Geochemical Society: Washington, DC, 2003; Vol. 54, pp 57−90.
(21) Wustman, B. A.; Morse, D. E.; Evans, J. S. *Langmuir* **2002**, *18*, 9901−9906.
(22) Zhang, B.; Wustman, B. A.; Morse, D. E.; Evans, J. S. *Biopolymers* **2002**, *63*, 358−369.
(23) Wustman, B. A.; Santos, R.; Zhang, B.; Evans, J. S. *Biopolymers* **2002**, *65*, 362−371.
(24) Perczel, A.; Hollosi, M.; Sandor, P.; Fasman, G. D. *Int. J. Pept. Protein Res.* **1993**, *41*, 223−236.
(25) Sreerama, N.; Woody, R. W. *Biochemistry* **1994**, *88*, 10022−10025.
(26) Ramirez-Alvarado, M.; Blanco, F. J.; Niemann, H.; Serrano, L. *J. Mol. Biol.* **1997**, *273*, 898−912.
(27) Lockwood, N. A.; van Tankeren, R.; Kayo, K. H. *Biomacromolecules* **2002**, *3*, 1225−1232.
(28) Shen, X.; Belcher, A. M.; Hansma, P. K.; Stucky, G. D.; Morse, D. E. *J. Biol. Chem.* **1997**, *272*, 32472−32481.

CG049919A